Aggregation methods in food chains with nutrient recycling

B.W. Kooi [a],[*], J.C. Poggiale [b], P. Auger [c], S.A.L.M. Kooijman [a]

[a] *Department of Theoretical Biology, Faculty of Earth and Life Sciences, Institute of Ecological Science, Vrije Universiteit, De Boelelaan 1087, 1081 HV Amsterdam, The Netherlands*
[b] *Centre D'Océanologie de Marseille, U.M.R. 6535, Campus de Luminy Case 901, 13288 Marseille Cedex 9, France*
[c] *Université Claude Bernard, Lyon 1, UMR CNRS 5558, 43 Bd du 11 Novembre 1918, 69622 Villeurbanne Cedex, France*

Abstract

This paper is devoted to the study of food chain models under batch and chemostat conditions where nutrient recycling is taken into account. The food chain is formed by a nutrient and two populations, prey and predator (producers and consumers). Species at both trophic levels digest their food source only partly. The unusable part of the food is ejected in the reactor as faeces together with metabolic products. The excreted material together with death material, detritus, is decomposed and this gives the recycling of the nutrient. In closed (batch-type environment) systems the elemental matter needed by producers must be provided through recycling where light energy from the environment supplies the necessary energy that fuels the life processes. In open (chemostat-type environment) systems this energy is added to the system via the chemical energy stored in the organic compounds in the inflow. Bifurcation analysis is used to study the effects of material recycling on the long-term dynamic behaviour of these simple food chains. An aggregation method is developed for situations in which each trophic level is characterized by differing time scales. This allows us to reduce the dimension of the model which gives good approximations after the fast transient. We will show that first-order approximations are needed in order to get the same qualitative long-term dynamics for both the full and the reduced model. © 2002 Elsevier Science B.V. All rights reserved.

Keywords: Aggregation methods; Batch reactor; Chemostat; Food chains; Nutrient recycling

1. Introduction

Recently it is found that effects of nutrient recycling plays an important role to the stability of ecosystems (DeAngelis, 1992). With nutrient recycling, waste-products and dead organisms from the biotic trophic levels are mineralised, possibly by a decomposer, into the abiotic nutrient. In the literature closed (batch-type environment) and open (chemostat-type environment) ecosystems are analysed.

In a batch reactor system the biological components and the nutrient are added to a closed system and thereafter the system is self-sustaining. In Nisbet and Gurney (1976) an elucidating model for carbon cycling in a closed ecosystem is described. In that model respiration products are converted directly to inorganic material, carbon

* Corresponding author. Tel.: +31-20-444-7129; fax: +31-20-444-7123

E-mail address: kooi@bio.vu.nl (B.W. Kooi).

dioxide CO_2, at a fixed rate proportional to the biomass of the population. This implies the assumption that the presence of decomposers does not significantly influence the rate of provision of material for decomposition and that decomposition is sufficiently fast to neglect time delays in the decomposition process.

In a chemostat there is a continuous flow of the nutrient through the reactor containing the populations. Chemostat conditions might resemble some ecosystems in a very simple model for a lake or other aquatic habitats, see also DeAngelis (1992). A nutrient–phytoplankton–zooplankton system is analysed in Beretta et al. (1990), Ruan (1993, 2001), where the nutrient is regenerated from dead biomass by bacterial decomposition. The dynamics of the decomposer is not modelled, however, a distributed time lag in the recycling is introduced to model time required to regeneration of the nutrient.

In this paper the production of degradable material at each trophic level occurs as side effects of three biological processes. These three processes involved in the living of each population are the assimilation, maintenance and growth process (Kooijman, 2000). Only a part of the food ingested by species is assimilated and the unusable parts are ejected in the reactor in the form of faeces. Subsequently, a part of the assimilated material is used for synthesis of new biomass and the other part forms products, associated with the maintenance and the growth process, that are excreted in the reactor. With our model formulation products are formed at two rates as waste-products by the three processes. The metabolic waste-products are assumed to be degraded instantaneously into nutrients. The other products such as faeces are degraded exponentially at a fixed recycle rate. These products yield extra state variables for each trophic level. Remark that, as in the papers mentioned sofar, the decomposers are not modelled explicitly.

One of our objective is to study the effects of material recycling on the long-term dynamic behaviour of these simple food chain. We perform a numerical bifurcation analysis for the chemostat case. The results are presented in bifurcation diagrams where regions in the parameter space are distinguished where qualitatively different asymptotic dynamics, equilibrium or cyclic behaviour, occurs.

Another aim is to obtain a better insight in the dynamical properties of the system by reducing the dimension. We use aggregation methods for this purpose. With perfect aggregation new global variables are defined which allows one to describe the dynamics of the system in a condensed way (Iwasa et al., 1987, 1989). In previous papers, we used perturbation techniques to perform approximate aggregation which have been applied to complex ecological models with different time scales (Auger et al., 2000a). The method works when the fast system possesses a stable equilibrium (Auger and Poggiale, 1996) and also with a stable limit cycle (Poggiale and Auger, 1996). Here we shall take advantage of the different time scales for the trophic levels of the food chain to apply aggregation methods (singular perturbation techniques) to simplify the models for the dynamics of the system.

In Rinaldi and Muratori (1992a,b), Muratori and Rinaldi (1989, 1992) a singular perturbation technique is applied to slow-fast systems. The model is the Rosenzweig–MacAthur model where the lowest trophic level grows logistically when not predated, that is nutrients are not modelled explicitly; they determine implicitly the carrying capacity. The trophic interactions are modelled using the Holling type II functional response. Different time-scales for the trophic levels is obtained by assuming a low efficiency for the trophic levels, that is, the maximum growth rate of each population is a small fraction of its maximum ingestion rate.

Since we study the effects of nutrient recycling we use a mass-balance model where the nutrients are modelled explicitly. We assume here complete recycling of the nutrients in the food chain. This facilitates the use of mass conservation laws with the formulation of the model. In Kooi et al. (1998), we applied aggregation methods to bi-trophic food chains under two environmental conditions, batch and chemostat, where the batch condition is a special case of the chemostat condition with dilution rate equal zero. The model was a mass-balance model where nutrients are modelled ex-

plicitly. We assumed different time scales for the trophic levels, but we kept the efficiencies at their normal magnitude. As a consequence, there is no complete time scale separation. The model analysed in Kooi et al. (1998) is a special case of the model analysed here with no maintenance and zero recycle rates of the faeces and metabolic products.

Community models (nutrient, prey, predator, materials and so on) are complex models involving many variables and parameters. The analytical analysis of these models is in general impossible. Usually, one has to perform bifurcation analysis with respect to one or two parameters only chosen among the great number of them. Aggregation methods allow to get a reduced model (1 or 2 dimensional in this paper) that can be studied analytically. In that case, we obtain general results on the complete model.

This paper is organized as follows. After the formulation of the model we describe different related models described and analysed in the literature. In the section on model analysis we first motivate the choice of the parameter values we use in our study. Thereafter we give short descriptions of the two mathematical techniques we use in analysing the model, namely bifurcation analysis and singular perturbation theory. We continue with the detailed analysis of the batch reactor and chemostat reactor cases. In both cases the full model as well as the aggregated model is analysed. In the Section 8 we relate the obtained results with those in the literature.

2. Model description

In this section, we give the model for a predator–prey–nutrient system in a closed or open environment with nutrient recycling. Thereafter the relationship with models proposed and analysed in the literature is described.

Food webs being a closed system are based on producers that convert carbon dioxide CO_2 to organic compounds. This process is carried out predominately by photosynthetic organisms that convert light energy to chemical energy; the chemical energy is stored within the organic compounds that are formed. These autotrophic organisms are plants in terrestrial systems and photosynthetic organisms such as the algae in marine systems. Most algae have also heterothrophic capabilities to supplement their energy and nutrient requirement and are called mixothrophs (Kooijman et al., 2002). The produced organic carbon becomes available to heterotrophic consumers. Hence, in closed systems, with no exchange of matter with the environment, energy is supplied to the system as light energy (solar radiation), otherwise the community will dissipate the available energy since biological processes are dissipative by the generation of waste heat, and therefore the community disappears. The waste heat leaves the system by convection or radiation.

In open systems consisting of heterotrophic organisms there is an input of allochthonous organic matter and chemical energy at the same time. No inflow of light energy is needed. When an autotroph or mixothroph is part of the food chain in an open system, light energy is supplied besides the chemical energy of the input matter, see also Kooijman et al. (2002). There is loss of energy via chemical energy in the matter that leaves the system and via convection or radiation of waste heat.

We assume that the reactor is spatially homogeneous and with a time-invariant input of the nutrient while all community components are washed-out at possibly different rates. In Fig. 1 the material fluxes through the food chain are depicted. We denote the nutrient concentration by x_0, prey biomass by x_1 and predator biomass by
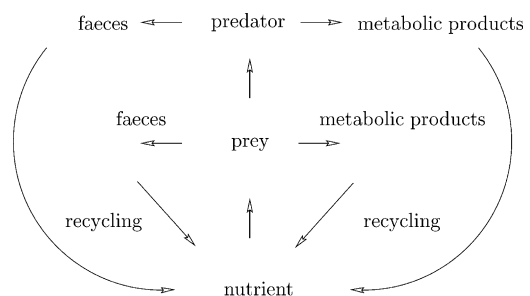

Fig. 1. Material fluxes through the nutrient–prey–predator food chain with recycling. Food is ingested and the unusable part is transferred into faeces. These faeces and the maintenance-associated metabolic products are recycled into nutrients.

x_2. The produced degradable materials excreted by the prey population are denoted by p_1 and z_1 and those produced by the predator population by p_2 and z_2. The model with nutrient recycling, reads:

$$\frac{dx_0}{d\tau} = (x_r - x_0)D_0 - I_{0,1}f_{0,1}(x_0)x_1 + \alpha_1 p_1 + \beta_1 z_1$$
$$+ \alpha_2 p_2 + \beta_2 z_2, \tag{1a}$$

$$\frac{dx_1}{d\tau} = \mu_{0,1}f_{0,1}(x_0)x_1 - m_1 x_1 - D_1 x_1$$
$$- I_{1,2}f_{1,2}(x_1)x_2, \tag{1b}$$

$$\frac{dx_2}{d\tau} = \mu_{1,2}x_2 f_{1,2}(x_1) - m_2 x_2 - D_2 x_2, \tag{1c}$$

$$\frac{dp_1}{d\tau} = ((I_{0,1} - \mu_{0,1})f_{0,1}(x_0)x_1 - \alpha_1 p_1) - D_1 p_1, \tag{1d}$$

$$\frac{dp_2}{d\tau} = ((I_{1,2} - \mu_{1,2})f_{1,2}(x_1)x_2 - \alpha_2 p_2) - D_2 p_2, \tag{1e}$$

$$\frac{dz_1}{d\tau} = m_1 x_1 - \beta_1 z_1 - D_1 z_1, \tag{1f}$$

$$\frac{dz_2}{d\tau} = m_2 x_2 - \beta_2 z_2 - D_2 z_2, \tag{1g}$$

where $f_{i-1,i}(x_{i-1})$ are the scaled Holling type II functional responses for $i = 1, 2$ defined by

$$f_{i-1,i}(x_{i-1}) = \frac{x_{i-1}}{k_{i-1,i} + x_{i-1}}. \tag{2}$$

The equations given above are derived by applying mass conservation laws for each compartment indicated in Fig. 2. See Tables 1 and 2 for a definition of the parameters. We assume $y_{i-1,i} = \mu_{i-1,i}/I_{i-1,i}$ to be constant, called the efficiency (ecology) or yield (microbiology). For biologically realistic situations some of the parameters are related as follows: $I_{i-1,i} > \mu_{i-1,i} > 0$, that is the efficiency is less than one ($y_{i-1,I} < 1$), and $0 \leq m_i < \mu_{i-1,i}$, that is the maintenance rate is less than maximum growth rate, while generally $\mu_{1,2} < \mu_{0,1}$.

We described now the terms in system Eqs. (1a), (1b), (1c), (1d), (1e), (1f) and (1g) one by one. The first term on the right-hand side of Eq. (1a) is the supply rate minus the removal rate of the nutrient into and from the reactor. The second term is the
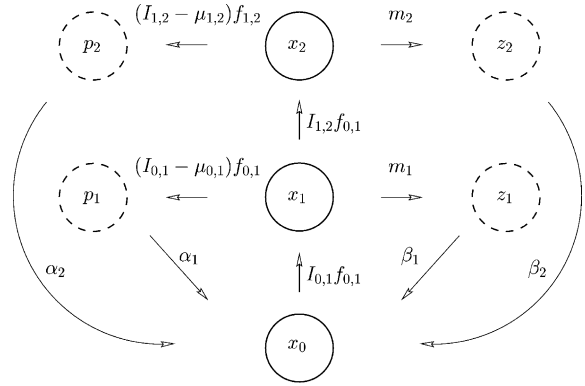

Fig. 2. Material fluxes through the food chain with recycling. Food is ingested with rate $I_{i-1,i}f_{i-1,i}x_i$. Per unit of time, the part $(I_{i-1,i} - \mu_{i-1,i})\,f_{i-1,i}x_i$ is unusable and transferred into faeces p_i. The faeces are decomposed at an exponential decay rate α_i. Maintenance-associated products z_i are formed at a rate $m_i x_i$. These products are decomposed at an exponential decay rate β_i.

Table 1
Parameters and state variables for both full and reduced model: t = time, m = biomass, v = volume of the region of interest

Parameter	Unit	Interpretation
t	t	Time
τ	t	Fast time variable
x_0	m v^{-1}	Nutrient density
x_i	m v^{-1}	Biomass density
p_i	m v^{-1}	Faeces
1_i	m v^{-1}	Metabolic product density
x_r	m v^{-1}	Nutrient concentration in reservoir
D	t^{-1}	Dilution rate
m_i	t^{-1}	Maintenance rate coefficient
$k_{i-1,i}$	m v^{-1}	Saturation constant
$I_{i-1,i}$	t^{-1}	Food uptake rate coefficient
$\mu_{i-1,i}$	t^{-1}	Population growth rate coefficient
$y_{i-1,i}$	–	Yield or efficiency
α_i	t^{-1}	Faeces recycle rate
β_i	t^{-1}	Metabolic products recycle rate

ingestion rate of the nutrient by the prey. The last four terms stand for the recycling rates of the faeces and metabolic products. The first terms on the right-hand side of Eqs. (1b) and (1c) are the growth rates, the second terms the production rate of the maintenance-associated products and the third terms the removal rate of the biomasses from the reactor. The last term in Eq. (1b) is the

Table 2
Parameter set for the substrate-bacterium-ciliate model ($\varepsilon = 1$) after Nisbet et al. (1983a), and the substrate-bacterium-worm model ($\varepsilon \ll 1$) after Kooi et al. (1998)

Parameter	Units	$i = 1$	$i = 2$	
			$\varepsilon = 1$	$\varepsilon \ll 1$
$y_{i-1,I}$	–	0.4	0.6	0.6
$\mu_{i-1,i}$	h^{-1}	0.5	0.2	0.01
$k_{i-1,I}$	Mg dm^{-3}	8	9	50

In both cases we have $I_{i-1,i} = \mu_{i-1,i}/y_{i-1,i}$ and $m_i = 0.05 \mu_{i-1,i}$. The values for the faeces recycle rates α_i, $i = 1, 2$ are taken equal to the maximum growth rate of the prey $\mu_{0,1}$. The nutrient density and the biomass density as well as the saturation constants $k_{i-1,i}$ measured in gram can be converted in C-mol for instance for glucose as the nutrient 30 g per C-mol glucose CH_2O, and 24.6 g dry weight per C-mol (Kooijman, 2000). Here we assume for simplicity that the chemical composition of the nutrient, prey and predator are the same.

ingestion rate of the prey by the predator. Since the predator is not consumed this term is missing in Eq. (1c). The first terms of Eqs. (1d) and (1e) are the formation rates of faeces which is proportional to the difference between the maximum ingestion rate and the maximum growth rate. The first terms of Eqs. (1f) and (1g) are the formation rate of the maintenance-associated products. We assume that the decomposers are abundant. Therefore they are not modelled explicitly and the materials released by the species in the reactor are degraded exponentially into nutrients. This gives the second terms $\alpha_i p_i$ in Eqs. (1d) and (1c), and $\beta_i z_i$ in Eqs. (1f) and (1g). Finally the removal rates of all products are the last terms of Eqs. (1d), (1e), (1f) and (1g).

Some terms in system Eqs. (1a), (1b), (1c), (1d), (1e), (1f) and (1g) may have different biological interpretations. For instance, m_i, $i = 1, 2$ are often called respiration rate constants and the D_i's are removal rates possibly due to natural death or wash-out.

The two environmental conditions considered in this paper are the batch reactor and the chemostat reactor. When $D_i = 0$, $i = 0, 1, 2$ there is no input of nutrients at the basis of the food chain nor output at all trophic levels. This describes the batch reactor. For this closed system no mass is

exchanged with the environment. On the other hand, when $D_i = D$, $i = 0, 1, 2$, the equations describe the dynamics of a food chain in a chemostat reactor where $D > 0$ is the dilution rate and $x_r > 0$ the concentration of the nutrient in the reservoir.

In this model formulation instantaneous recycling of the respiratory products and the faeces is obtained by assuming a fast nutrient recycling rate, that is $\alpha_i \gg \mu_{i-1,i}$ and $\beta_i \gg \mu_{i-1,I} > m_i$. Then, the last four equations Eqs. (1d), (1e), (1f) and (1g) give

$$\alpha_1 p_1 = (I_{0,1} - \mu_{0,1})f_{0,1}(x_0)x_1, \tag{3a}$$

$$\alpha_2 p_2 = (I_{1,2} - \mu_{1,2})f_{1,2}(x_1)x_2, \tag{3b}$$

$$\beta_1 z_1 = m_1 x_1, \tag{3c}$$

$$\beta_2 z_2 = m_2 x_2, \tag{3d}$$

where we used that D_i are negligible small with respect to α_i and β_i for $i = 1, 2$. These expressions must be substituted in Eq. (1a). The resulting equation together with Eqs. (1b) and (1c) form the reduced model for the predator-prey system in the chemostat. Here we will assume that $\beta_i = \infty$, $i = 1$, 2, that is instantaneous degradation of the labile maintenance-associated products and we neglect natural death. We take $0 < \alpha_i < \infty$, that is the particulate nutrients are regenerated by decomposers which are assumed to be available ad libitum, so that we do not model their dynamics explicitly. Notice that when $\alpha_i = \beta_i = 0$, $i = 1, 2$ the model boils down to the predator–prey model without recycling analysed in Kooi et al. (1998).

In the next section, we will use aggregation techniques to derive reduced systems of the following full system where ε enforces time-separation

$$\frac{dx_0}{d\tau} = (x_r - x_0)D_0 - I_{0,1}f_{0,1}(x_0)x_1 + \alpha_1 p_1 + m_1 x_1 + \alpha_2 p_2 + \varepsilon m_2 x_2, \tag{4a}$$

$$\frac{dx_1}{d\tau} = \mu_{0,1}f_{0,1}(x_0)x_1 - m_1 x_1 - D_1 x_1 - \varepsilon I_{1,2}f_{1,2}(x_1)x_2, \tag{4b}$$

$$\frac{dx_2}{d\tau} = \varepsilon(\mu_{1,2}x_2 f_{1,2}(x_1) - m_2 x_2) - D_2 x_2, \tag{4c}$$

$$\frac{\mathrm{d}p_1}{\mathrm{d}\tau} = (I_{0,1} - \mu_{0,1})f_{0,1}(x_0)x_1 - \alpha_1 p_1 - D_1 p_1, \quad (4d)$$

$$\frac{\mathrm{d}p_2}{\mathrm{d}\tau} = \varepsilon(I_{1,2} - \mu_{1,2})f_{1,2}(x_1)x_2 - \alpha_2 p_2 - D_2 p_2. \quad (4e)$$

Notice that the incorporation of the time-scale effects, modelled in the same way as in the previous paper Kooi et al. (1998), differs from that done in Rinaldi and Muratori (1992a,b), Muratori and Rinaldi (1989, 1992). In those papers the maximum ingestion rate of the predator, $I_{1,2}$, is not multiplied with ε, only the maximum growth rate, $\mu_{1,2}$, is. The implication is that in their model the efficiency decreases down to zero when $\varepsilon \to 0$. This is hard to understand from a biochemical point of view; net conversion efficiencies from one organism to another are typically around 0.1, and from suitable organic substrate such as glucose to organism about 0.5 (Kooijman, 2000). We keep the conversion efficiency constant and multiply the maximum ingestion rate of the predator $I_{1,2}$, the maximum growth rate $\mu_{1,2}$ and the specific maintenance rate m_2 with ε. In this way the efficiency remains unchanged when ε is varied.

3. Model analysis

3.1. Parameter values

The full model Eqs. (4a), (4b), (4c), (4d) and (4e) will be analysed using numerical bifurcation analysis. The parameter values are after Nisbet et al., 1983a and given in Table 2. They are realistic for a two-trophic microbial food chain consisting of substrate, bacterium and ciliate. The values for the new parameters, the faeces recycle rates α_i are assumed to be the same as the maximum growth rate of the bacterium. The results are presented in one-parameter and two-parameter bifurcation diagrams. In a one-parameter bifurcation diagram the equilibrium biomass or extreme values during a limit cycle, are plotted as function of one bifurcation parameter for instance the nutrient input, whereby all other parameters are held constant. Parameter values at which the asymptotic dynamic

behaviour changes suddenly, fix bifurcation points.

In some realistic cases, like a food chain of sewage-bacterium-worm (for example the water nymph *Nais elinguis*, a oligochaete species) often found in waste-water treatment plants (Ratsak et al., 1993), there are differences in the order of magnitudes of the ingestion and growth rates. Parameter values for this model are also given in Table 2 and will be used when we do simulations associated with the aggregation technique.

3.2. Bifurcation analysis

For an introduction to bifurcation analysis the reader is referred to Guckenheimer and Holmes (1985), Kuznetsov (1998) and to Bazykin (1998) for the application to ecosystem models. Bifurcation analysis gives information about the long-term dynamic behaviour of nonlinear dynamic systems. The structural stability is studied with respect to so-called free or bifurcation parameters. When such a parameter is varied, a value at which the asymptotic dynamics changes abruptly (for instance the solution becomes a stable limit cycle instead of a stable equilibrium) is called a bifurcation point. Numerical bifurcation packages, such as auto: (Doedel et al., 1997) and locbif, content: (Khibnik et al., 1993; Kuznetsov and Levitin, 1997; Kuznetsov, 1998) are available to calculate bifurcation points.

Two bifurcations types appear to be important with the study of our model: the transcritical bifurcation which determines the boundary of coexistence of species in the parameter space and the Hopf bifurcation at which point the equilibrium of the system becomes unstable and the asymptotic dynamics becomes oscillatory. The phenomenon that the system becomes unstable at higher levels of nutrient supply was found by Rosenzweig (1971) with the Rosenzweig–MacArthur model for a predator–prey system and is known as the paradox of enrichment. Thereafter it was found analysing many related predator–prey models under various environmental conditions. Generally, the system not only starts to oscillate, but these oscillations become also severe.

A wide class of predator–prey models possess similar bifurcation diagrams, see for instance Nisbet et al. (1983b), Gurney and Nisbet (1998). In these bifurcation diagrams the long-term dynamics is studied depending on environmental conditions. For the batch reactor the nutrient availability at the start of the experiment and the removal rate (due to harvesting or mortality) of the predator are often used as bifurcation parameters. In the chemostat case the natural bifurcation parameters are the concentration of the nutrients in the inflow and the dilution rate.

3.3. Singular perturbation theory

In this section we give a short overview of singular perturbation techniques. The reader is referred to Hoppensteadt (1993), Jones (1995), Kevorkian and Cole (1995) for introductions into perturbation theory. Singular perturbation theory deals with systems of the following form:

$$\frac{dx}{d\tau} = f(x, y, \varepsilon), \tag{5a}$$

$$\frac{dy}{d\tau} = \varepsilon g(x, y), \tag{5b}$$

where $x(0) = x_0$ and $y(0) = y_0$. This system Eqs. (5a) and (5b) can be reformulated with a change of time-scale as

$$\varepsilon \frac{dx}{dt} = f(x, y, \varepsilon), \tag{6a}$$

$$\varepsilon \frac{dy}{dt} = \varepsilon g(x, y), \tag{6b}$$

where $t = \varepsilon\tau$. Notice that in the singular perturbation problem when ε is put equal to zero in Eqs. (6a) and (6b), these equations have a structural different form than the unperturbed original system.

The first step consists in setting $\varepsilon = 0$ which gives the set of fast equilibria. In the first case, the *fast system* Eqs. (5a) and (5b), we get the fast system $d\bar{x}/d\tau = f(\bar{x}, \bar{y}, 0)$ and $d\bar{y}/d\tau = 0$. The equilibria of this fast system are given by: $f(\bar{x}, \bar{y}, 0) = 0$.

In the second case, the *slow system* Eqs. (6a) and (6b), we get the algebraic equation of the so called

'slow manifold': $f(\bar{x}, \bar{y}, 0) = 0$. With good hypothesis, this is equivalent to $\bar{x} = h(\bar{y})$ and we can then substitute $\bar{x}$ by $h(\bar{y})$ in the second equation, then: $d\bar{y}/dt = g(h(\bar{y}), \bar{y})$ where generally $\bar{x}(0) \neq h(\bar{y}(0))$. Observe that we divided by ε by derivating with respect to t instead of τ. The procedure is generally mathematically justified by the Tikhonov theorem (Tikhonov et al., 1985), which guarantees that the solution $\bar{x}(t)$, $\bar{y}(t)$ is a good approximation for $x(t)$, $y(t)$ in some finite time interval when ε is sufficiently small.

In this paper, we use a geometrical approach. The set of equilibria $M_0 = \{(x, y); f(x, y, 0) = 0\}$ defined for $\varepsilon = 0$ is an attracting invariant set in the phase space, and is assumed to be a manifold. When ε is positive, but small, we want to know if the previous attracting invariant manifold persists and how to calculate the dynamics on the perturbated attracting invariant manifold M_ε. The theory of normally hyperbolic invariant manifolds (Fenichel, 1971; Hirch et al., 1977; Wiggins, 1994) aims to answer this kind of questions, by the way of a geometrical approach. The condition of persistence is given by the normal hyperbolicity. It means that under the dynamics linearized about the invariant manifold, the growth rate of vectors transverse to the invariant manifold dominates the growth rate of vectors tangent to the invariant manifold.

In some cases, there are multiple equilibria for the fast system, some are stable, the other are unstable. Here, we will deal with the case where there are two equilibria for which the stability condition depends on the value of the slow variables. After the fast transient, because of the dynamics of the slow variables, the stability of the two fast equilibria switches. At the bifurcation point, the invariant manifold is not normally hyperbolic. In (Dumortier and Roussarie, 1996, 2000), the authors propose a geometrical approach to deal with such non-hyperbolic singularities. Their idea consists in successive blows-up until the singularity becomes hyperbolic. Roughly speaking, there are two invariant manifolds for $\varepsilon = 0$, one for each stable set of equilibria. For small positive ε, the dynamics starts at one and suddenly it moves fast to the other one and continues there, leading to an attractor (Auger et

al., 2000b) or following the manifold until it becomes unstable. In the latter case it jumps suddenly to the first slow manifold again, and so on leading to a quasi-limit cycle. An example is dealt with in Kooi et al. (1998).

The main steps of the aggregation method based on the Fenichel theorem are:

1) Find the equilibria of the fast system ($\varepsilon = 0$) defined by $f(x, y, 0) = 0$.
2) Analyse the linear stability of the equilibria. For each y, the stability depends on y.
3) If for a given y, the equilibrium is hyperbolically stable, then substitute this equilibrium value in the equation of the derivative of y, dy/dt. If for a given y, the equilibrium is non-hyperbolically stable, then one should use the method developed in Dumortier and Roussarie (1996). In this paper, we only deal with the hyperbolic case. A forthcoming paper will be devoted to the non-hyperbolic case.

4. Batch reactor conditions

The model under batch conditions, that is a closed system with no material exchange with the environment, is obtained from model Eqs. (4a), (4b), (4c), (4d) and (4e) with $D_i = 0$, $i = 0, 1, 2$. The total biomass, for instance measured in C-mol, denoted by C and defined by

$$C(t) = x_0(t) + x_1(t) + p_1(t) + x_2(t) + p_2(t), \tag{7}$$

is time-invariant, $C(t) = C(0)$, due to mass conservation. This equality will be used to eliminate the variable x_0. By replacing x_0 by $C - x_1 - p_1 - x_2 - p_2$, system Eqs. (4a), (4b), (4c), (4d) and (4e) with $D_i = 0$, $i = 0, 1, 2$, reads:

$$\frac{dx_1}{d\tau} = x_1 \left(\mu_{0,1} \frac{C - x_1 - p_1 - x_2 - p_2}{k_{0,1} + C - x_1 - p_1 - x_2 - p_2} - m_1 \right) - \varepsilon I_{1,2} \frac{x_1 x_2}{k_{1,2} + x_1}, \tag{8a}$$

$$\frac{dx_2}{d\tau} = \varepsilon x_2 \left(\mu_{1,2} \frac{x_1}{k_{1,2} + x_1} - m_2 \right), \tag{8b}$$

$$\frac{dp_1}{d\tau} = (I_{0,1} - \mu_{0,1})$$

$$\times \frac{C - x_1 - p_1 - x_2 - p_2}{k_{0,1} + C - x_1 - p_1 - x_2 - p_2} x_1 - \alpha_1 p_1, \tag{8c}$$

$$\frac{dp_2}{d\tau} = \varepsilon(I_{1,2} - \mu_{1,2}) \frac{x_1}{k_{1,2} + x_1} x_2 - \alpha_2 p_2. \tag{8d}$$

This makes it possible to deal with the four dimensional full system for the state variables x_1, x_2, p_1, p_2, where C is used as a bifurcation parameter. Notice that we assumed recycling, that is $\alpha_i > 0$, $i = 1, 2$. When $\alpha_i = 0$, the variables p_1, p_2 do not appear in any of the two Eqs. (8a) and (8b) when C is defined as in Kooi et al. (1998) by

$$C(t) = x_0(t) + \frac{x_1(t)}{y_{0,1}} + \frac{x_2(t)}{y_{0,2}}, \tag{9}$$

where $y_{i-1,i} = \mu_{i-1,i}/I_{i-1,i}$ is the efficiency again. We introduced $y_{0,2} = y_{0,1}y_{1,2}$. We remark that the total biomass is here measured in gram instead of C-mol in Eq. (7). The converted factor is for instance for glucose as the nutrient 30 g per C-mol glucose CH_2O, and 24.6 g dry weight per C-mol biomass $CH_{1.8}N_{0.2}O_{0.5}$ (Kooijman, 2000).

Thus, without recycling the first two equations

$$\frac{dx_1}{d\tau} = x_1 \left(\mu_{0,1} \frac{C - x_1/y_{0,1} - x_2/y_{0,2}}{k_{0,1} + C - x_1/y_{0,1} - /y_{0,2}} - m_1 \right) - \varepsilon I_{1,2} \frac{x_1 x_2}{k_{1,2} + x_1}, \tag{10a}$$

$$\frac{dx_2}{d\tau} = \varepsilon x_2 \left(\mu_{1,2} \frac{x_1}{k_{1,2} + x_1} - m_2 \right), \tag{10b}$$

can be solved separately and then

$$\frac{dp_1}{d\tau} = (I_{0,1} - \mu_{0,1})$$

$$\times \frac{C - x_1/y_{0,1} - x_2/y_{0,2}}{k_{0,1} + C - x_1/y_{0,1} - x_2/y_{0,2}} x_1, \tag{11a}$$

$$\frac{dp_2}{d\tau} = \varepsilon(I_{1,2} - \mu_{1,2}) \frac{x_1}{k_{1,2} + x_1} x_2. \tag{11b}$$

are used to obtain $p_1(t)$, $p_2(t)$. Hence, although products are also formed when no recycling is

involved, we nevertheless can apply a mass-conservation argument, see Smith and Waltman (1994), to reduced the dimension of the system with the biomasses a state variables, by one.

The equilibria of the full system Eqs. (8a), (8b), (8c) and (8d) with $\varepsilon = 1$ are

$$x_1^* = \frac{k_{1,2}m_2}{\mu_{1,2} - m_2}, \tag{12a}$$

$$x_2^* = \frac{k_{1,2} + x_1^*}{I_{1,2}}$$
$$\times \left(\mu_{0,1} \frac{C - x_1^* - p_1^* - x_2^* - p_2^*}{k_{0,1} + C - x_1^* - p_1^* - x_2^* - p_2^*} - m_1 \right), \tag{12b}$$

$$p_1^* = \frac{(I_{0,1} - \mu_{0,1})m_1}{\mu_{0,1}\alpha_1} x_1^*, \tag{12c}$$

$$p_2^* = \frac{(I_{1,2} - \mu_{1,2})m_2}{\mu_{1,2}\alpha_2} x_2^*, \tag{12d}$$

where x_2^* is still given implicitly where the positive root of the resulting quadratic equation is taken.

The total biomass C defined in Eq. (7) has to be sufficient high to get coexistence of prey or even both prey and predator in the reactor. The value of C at the boundary of the region with coexistence, is called a transcritical bifurcation TC, one where only the prey can persist and one where the predator can persist too.

Mathematically the first point is found when the following conditions are satisfied. The equilibrium with biomass of the prey is zero, $\hat{x}_1 = \hat{x}_2 = 0$, is such that the growth rate of the prey is zero too, $dx_1/d\tau = 0$. That is, we are at the boundary of the region where the prey can invade the nutrient system. Eqs. (8c) and (8d) give $\hat{p}_1 = \hat{p}_2 = 0$. The resulting equations are

$$\hat{C} = \hat{x}_0, \tag{13a}$$
$$0 = \mu_{0,1}f_{0,1}(\hat{x}_0) - m_1. \tag{13b}$$

These two equations for the positive equilibrium values $\hat{x}_0$ fix the value $\hat{C}$. We obtain

$$\hat{C} = \hat{x}_0 = \frac{k_{0,1}m_1}{\mu_{0,1} - m_1}. \tag{14}$$

At the second transcritical bifurcation that marks the point where the predator can invade the nutrient–prey system, the equilibrium with biomass of the predator is zero, $\tilde{x}_2 = 0$ and furthermore the growth rate of the predator is zero too, $dx_2/d\tau = 0$. Eq. (8d) gives directly $\tilde{p}_2 = 0$. The resulting equations are

$$\tilde{C} = \tilde{x}_0 + \tilde{x}_1 + \tilde{p}_1, \tag{15a}$$
$$0 = \mu_{0,1}f_{0,1}(\tilde{x}_0) - m_1, \tag{15b}$$
$$0 = \mu_{1,2}f_{1,2}(\tilde{x}_1) - m_2, \tag{15c}$$
$$0 = (I_{0,1} - \mu_{0,1})f_{0,1}(\tilde{x}_0)\tilde{x}_1 - \alpha_1\tilde{p}_1. \tag{15d}$$

Eqs. (15a), (15b), (15c) and (15d) give

$$\tilde{x}_0 = \frac{k_{0,1}m_1}{\mu_{0,1} - m_1}, \tag{16a}$$

$$\tilde{x}_1 = \frac{k_{1,2}m_2}{\mu_{1,2} - m_2}, \tag{16b}$$

$$\tilde{p}_1 = \frac{(I_{0,1} - \mu_{0,1})m_1\tilde{x}_1}{\mu_{0,1}\alpha_1}. \tag{16c}$$

Eq. (15a) is a consequence of complete recycling of the nutrients which gives conservation, in this case in absence of the predator. Substitution of Eqs. (16a), (16b) and (16c) in Eq. (15a) gives the transcritical bifurcation value $\tilde{C}$.

When increasing C, system Eqs. (8a), (8b), (8c) and (8d) shows a Hopf bifurcation which marks the origin of oscillatory behaviour. No closed form expressions are available and we have to calculate this point numerically.

5. Two time scales batch reactor case

In this section, we study the case with two different time scales, that is small ε. The fast system is obtained by putting $\varepsilon = 0$ in system Eqs. (8a), (8b), (8c) and (8d). It is formed by Eqs. (8a), (8c) and (8d) where $\bar{x}_2$ is treated as a parameter.

$$\frac{d\bar{x}_1}{d\tau} = \bar{x}_1 \left(\mu_{0,1} \frac{C - \bar{x}_1 - \bar{p}_1 - \bar{x}_2 - \bar{p}_2}{k_{0,1} + C - \bar{x}_1 - \bar{p}_1 - \bar{x}_2 - \bar{p}_2} - m_1 \right), \tag{17a}$$

$$\frac{d\bar{p}_1}{d\tau} = (I_{0,1} - \mu_{0,1})$$

$$\times \frac{C - \bar{x}_2 - \bar{p}_2 - \bar{x}_1 - \bar{p}_1}{k_{0,1} + C - \bar{x}_2 - \bar{p}_2 - \bar{x}_1 - \bar{p}_1} \bar{x}_1$$

$$- \alpha_1 \bar{p}_1, \tag{17b}$$

$$\frac{d\bar{p}_2}{d\tau} = -\alpha_2 \bar{p}_2. \tag{17c}$$

The equilibria of this three-dimensional system for the three fast variables $\bar{x}_1$, $\bar{p}_1$ and $\bar{p}_2$ read

$$\bar{x}_1^* = \frac{\mu_{0,1}\alpha_1(C - \bar{x}_2 - \hat{C})}{m_1(I_{0,1} - \mu_{0,1}) + \mu_{0,1}\alpha_1}, \tag{18a}$$

$$\bar{p}_1^* = \frac{(I_{0,1} - \mu_{0,1})m_1}{\mu_{0,1}\alpha_1} \bar{x}_1^*, \tag{18b}$$

$$\bar{p}_2^* = 0, \tag{18c}$$

where $\bar{x}_2$ is the slow variable of which the dynamics is described by an ordinary differential equation (ode) derived below.

Because the ode Eq. (17c) for $\bar{p}_2$ is decoupled from the two odes Eqs. (17a) and (17b), it is sufficient to study their 2×2 Jacobian matrix evaluated at the equilibrium $\bar{x}_1$ and $\bar{p}_1$ given in Eqs. (18a) and (18b). It can be shown that

i) If $C < \hat{C} + \bar{x}_2$ the equilibrium $(\bar{x}_1; \bar{p}_1; \bar{p}_2) = (0; 0; 0)$ is stable and is the unique non-negative equilibrium.
ii) If $\hat{C} + \bar{x}_2 < C$ the trivial equilibrium $(\bar{x}_1; \bar{p}_1; \bar{p}_2) = (0; 0; 0)$ is unstable and the non-trivial $(\bar{x}_1; \bar{p}_1; \bar{p}_2) = (\bar{x}_1^*; \bar{p}_1^*; 0)$ is stable and is the unique positive equilibrium.

These equilibria Eq. (18a) for x_1, Eq. (18b) for p_1 and Eq. (18c) for p_2, where $\bar{x}_2$ is a parameter, is substituted in Eq. (8b) with $\varepsilon = 0$. This yields the slow system for the slow variable $\bar{x}_2$ when $\bar{x}_1 > 0$.

$$\frac{d\bar{x}_2}{dt} = \bar{x}_2 \left(\mu_{1,2} \frac{\bar{x}_1}{k_{1,2} + \bar{x}_1} - m_2 \right), \tag{19}$$

Or when $\bar{x}_1 \leq 0$

$$\frac{d\bar{x}_2}{dt} = -m_2 \bar{x}_2. \tag{20}$$

where $t = \varepsilon\tau$ again. The equilibrium is

$$\bar{x}_2^* = C - \frac{m_1 k_{0,1}}{\mu_{0,1} - m_1} - \frac{m_1(I_{0,1} - \mu_{0,1}) + \mu_{0,1}\alpha_1}{\mu_{0,1}\alpha_1}$$

$$\times \frac{m_2 k_{1,2}}{\mu_{1,2} - m_2}$$

$$= C - \tilde{C}, \tag{21}$$

where we used Eqs. (16a), (16b) and (16c). We conclude that

i)   If $C < \hat{C}$ then $(\bar{x}_1; \bar{x}_2; \bar{p}_1; \bar{p}_2)$ approaches $(0; 0; 0; 0)$.
ii) If $\hat{C} < C < \tilde{C}$ then $(\bar{x}_1; \bar{x}_2; \bar{p}_1; \bar{p}_2)$ approaches $(\bar{x}_1^*; 0; \bar{p}_1^*; 0)$.
iii) If $\tilde{C} < C$ then $(\bar{x}_1; \bar{x}_2; \bar{p}_1; \bar{p}_2)$ approaches $(\bar{x}_1^*; \bar{x}_2^*; \bar{p}_1^*; 0)$.

The points at which the reduced model changes, fixed by $C = \hat{C}$ and $C = \tilde{C}$ are transcritical bifurcation points for both the reduced model and the full model given in Eqs. (15a), (15b), (15c), (15d), (16a), (16b) and (16c). With respect to this, the reduced model reflects the asymptotic dynamics of the full model well.

In Figs. 3 and 4 simulation results for the prey and predator biomass densities, $x_1(\tau)$, $x_2(\tau)$, and for the nutrient density, $x_0(\tau)$, are depicted for the reduced and full model where $C = 300 > \tilde{C}$. After the transient, the solution of the reduced model is close to that of the full model. The differences for the equilibria of both models is explained as follows. Comparing Eqs. (8b) and (19) gives that in equilibrium we have $\bar{x}_1^* = x_1^*$ and subsequently $\bar{p}_1^* = p_1^*$, see Eqs. (8c) and (18b). The difference between $\bar{x}_2^*$ and x_2^* is due to the fact that the consumption term of the predator feeding on the prey, $(\varepsilon I_{1,2}x_1/(k_{1,2}+x_1))x_2$ is neglected in Eq. (17a) and not in Eq. (8a). After $\tau \approx 600$, the biomass density of the predator $x_2(\tau)$ is large and this explains the difference between $\bar{x}_2^*$ and x_2^*, and partly the difference between $\bar{p}_2^*$ Eq. (18c) and p_2^* Eq. (12d). Furthermore we have $\bar{x}_0^* = \hat{C}$ and therefore $\bar{x}_0^*$ is time-invariant. This follows directly from substitution of the expressions Eqs. (18a), (18b) and (18c) in the expression for C in Eq. (7). This explains the difference between $\bar{x}_0^*$ and x_0^* in Fig. 4.
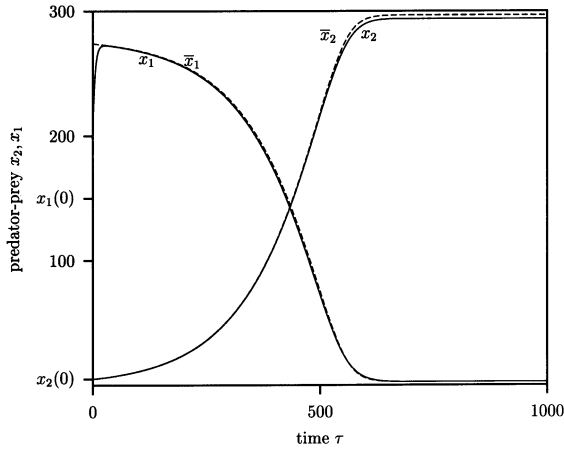
Fig. 3. The biomasses of the predator and prey for the full system x_2, x_1 and the reduced system $\bar{x}_2$, $\bar{x}_1$ as a function of time t, with $C = 300$ and initial conditions: $x_0(0) = 145$, $x_1(0) = 150$, $p_1(0) = 0$, $x_2(0) = \bar{x}_2(0) = 5$ and $p_2(0) = 0$. Solid lines are for the full system $x_i(t)$, and dashed lines are for the reduced system $\bar{x}_i(t)$, $i = 1, 2$.
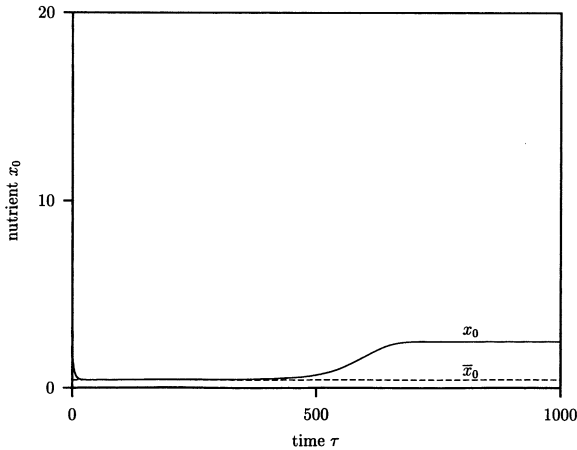

Fig. 4. The nutrient density for the full system x_0 and the reduced system $\bar{x}_0$ as a function of time t, with $C = 300$. Initial conditions as in Fig. 3 thus $x_0(0) = 145$. Solid lines are for the full system $x_0(t)$ and dashed lines are for the reduced system $\bar{x}_0(t)$.

When $\varepsilon > 0$ there is a C so that the full system has a Hopf bifurcation. In Fig. 5 we depict the two-parameter bifurcation diagram where C and ε are the bifurcation parameters. The curve denoted by H is the Hopf bifurcation curve that approaches the $\varepsilon = 0$ axis when $C \to \infty$. Hence, for a fixed strictly positive value of ε and when C is
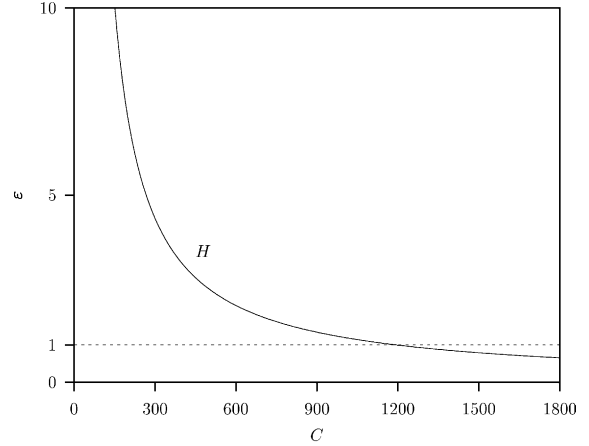

Fig. 5. Two-parameter bifurcation diagram for the model under the batch conditions Eqs. (8a), (8b), (8c) and (8d). The bifurcation parameters are ε and the initial biomass in the reactor C. Values assigned to physiological parameters and reference values for the perturbation parameters are listed in Table 2. The curve H marks a supercritical Hopf bifurcation curves.

greater than its value on the H-curve (1200 in Fig. 5), the reduced system has a stable equilibrium, as is shown in this section, while the full system converges to a stable limit cycle when time goes to infinity. In other words, the approximation is valid for a very small ε when C is large.

This illustrates that for practical cases when $\varepsilon > 0$, the reduced system gives not always good approximations for the long-term dynamics. In the next section, we deal with the chemostat case where we retain first-order terms with the construction of a reduced model. This gives a better long-term approximation. Such an approach can be applied with batch conditions discussed here in the same manner.

6. Chemostat conditions

The model under chemostat conditions, is obtained from model Eqs. (4a), (4b), (4c), (4d) and (4e) with $D_i = D$, $i = 0$, 1, 2. We define now the total biomass measured in C-mol $H(t)$ by

$$H(t) = x_0(t) + x_1(t) + x_2(t) + p_1(t) + p_2(t). \quad (22)$$

By replacing x_0 by $H - x_1 - p_1 - x_2 - p_2$, system

Eqs. (4a), (4b), (4c), (4d) and (4e) with $D_i = D$, $i = 0, 1, 2$, reads:

$$\frac{dH}{d\tau} = -\varepsilon D(H - x_r), \tag{23a}$$

$$\frac{dx_1}{d\tau} = x_1 \left(\mu_{0,1} \frac{H - x_1 - p_1 - x_2 - p_2}{k_{0,1} + H - x_1 - p_1 - x_2 - p_2} - m_1 \right.$$
$$\left. - \varepsilon D - \varepsilon I_{1,2} \frac{x_2}{k_{1,2} + x_1} \right), \tag{23b}$$

$$\frac{dx_2}{d\tau} = \varepsilon x_2 \left(\mu_{1,2} \frac{x_1}{k_{1,2} + x_1} - m_2 - D \right), \tag{23c}$$

$$\frac{dp_1}{d\tau} = (I_{0,1} - \mu_{0,1})$$
$$\times \frac{H - x_2 - p_2 - x_1 - p_1}{k_{0,1} + H - x_2 - p_2 - x_1 - p_1} \, x_1 - \alpha_1 p_1$$
$$- \varepsilon D p_1, \tag{23d}$$

$$\frac{dp_2}{d\tau} = \varepsilon (I_{1,2} - \mu_{1,2}) \frac{x_1}{k_{1,2} + x_1} \, x_2 - \alpha_2 p_2$$
$$- \varepsilon D p_2. \tag{23e}$$

First we analyse this model where $\varepsilon = 1$ with numerical bifurcation techniques. The two-parameter bifurcation diagram for the model with and without nutrient recycling is given in Fig. 6. The transcritical bifurcation curve which determines the boundary of coexistence of species in the parameter space is denoted by TC_r and the Hopf bifurcation curve, that bounds the region where the system oscillates, is denoted by H_r. We recall that the parameter values given in Table 2 are from Nisbet et al., 1983a. The transcritical bifurcation curve TC and Hopf bifurcation curve H are the two bifurcation curves for that model without nutrient recycling, thus $\alpha_1 = \alpha_2 = 0$.

For a fixed dilution rate the density of the nutrient in the inflow has to be sufficiently high to get coexistence of both prey and predator in the reactor. Equations similar to those for the batch reactor Eqs. (15a), (15b), (15c) and (15d), describe this transcritical bifurcation. The following substitutions have to be made: $C \rightarrow H$ and $m_i \rightarrow m_i + D$ and $\alpha_1 \rightarrow \alpha_1 + D$. In this way we obtain now a relationship between the two parameters D and x_r,
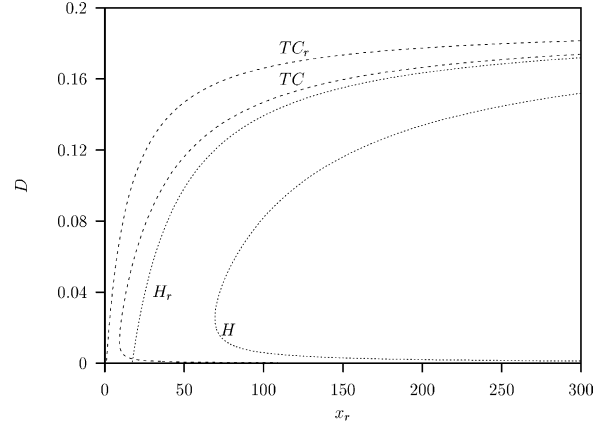

Fig. 6. Two-parameter bifurcation diagram for the predator–prey model in the chemostat with ($\alpha_1 = \alpha_2 = 0.5$) and without ($\alpha_1 = \alpha_2 = 0$) recycling Eqs. (23a), (23b), (23c), (23d) and (23e). The bifurcation parameters are the dilution rate D and the nutrient concentration in reservoir x_r. Values assigned to physiological parameters and reference values for the perturbation parameters are listed in Table 2. The curves TC, TC_r mark transcritical bifurcation curves, H and H_r mark supercritical Hopf bifurcation curves.

that is, the function $\tilde{x}_r(D)$ of which the graph is the bifurcation curve TC_r in Fig. 6.

When the nutrient supply is increased further, the positive equilibrium becomes unstable at a Hopf bifurcation H and a stable limit cycle originates. At that point the real part of two complex conjugate eigenvalues equals zero. Explicit expressions for the relationship between the two parameters D and x_r do not exist. Therefore, the Hopf bifurcation curve has to be approximated numerically.

In Fig. 7 the long-term biomass values for the predator x_2 are depicted as a function of x_r for a fixed $D = 0.08$. If x_r is lower that its transcritical bifurcation TC_r value the prey is the only organism in the reactor. If the x_r-values is higher than its TC_r-value the predator can invade the system when it is introduced in small amounts and there is a stable coexistence. When x_r is increased and the H_r-value is reached, this equilibrium becomes unstable. For higher x_r values the system oscillates and the maximum and minimum values of the stable limit cycles are plotted in Fig. 7. With rather high x_r values the minimum values become very low. For comparison in Fig. 7 results are also
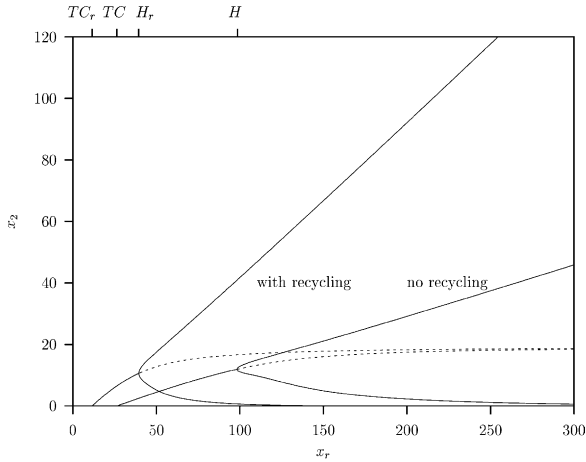
Fig. 7. One-parameter bifurcation diagram for the predator–prey model in the chemostat with ($\alpha_1 = \alpha_2 = 0.5$) and without ($\alpha_1 = \alpha_2 = 0$) recycling Eqs. (23a), (23b), (23c), (23d) and (23e). The bifurcation parameter is the nutrient concentration in reservoir x_r where $D = 0.08$. Values assigned to physiological parameters and reference values for the perturbation parameters are listed in Table 2. Solid curves are the stable equilibria and the extreme values of the stable limit cycles. Dashed curves indicate the unstable equilibria.

given for the nutrient-prey-predator model without recycling, $\alpha_1 = \alpha_2 = 0$, also for $D = 0.08$.

7. Two time scales chemostat reactor case

We will now apply the singular perturbation theory in the case that the prey dynamics feeding on nutrient is fast and that the predator dynamics feeding on the prey is slow ($\varepsilon \ll 1$) is formed by the two odes Eqs. (23b) and (23d). We will consider a zero-order approximation and a first-order approximation where all ε terms are retained. The bifurcation analysis of the resulting fast system can be done analytically for the zero-order approximation. For the first-order approximation we have to resort to calculated bifurcation diagrams.

7.1. Zero-order approximations

The fast system is exactly the same as in the batch reactor case Eqs. (17a), (17b) and (17c) where constant C has to be replaced by $\bar{H}$ which is

now an extra parameter, and we introduce $\hat{H} = \hat{C} = m_1 k_{0,1}/(\mu_{0,1} - m_1)$.

The two dimensional slow system for the variables $\bar{H}$ and $\bar{x}_2$ reads

$$\frac{d\bar{H}}{dt} = -D(\bar{H} - x_r), \tag{24a}$$

$$\frac{d\bar{x}_2}{dt} = \bar{x}_2\left(\mu_{1,2}\frac{\bar{x}_1}{k_{1,2} + \bar{x}_1} - m_2 - D\right), \tag{24b}$$

where for $\bar{x}_1$ the expression Eq. (18a) is substituted. Similar to the batch case we introduce

$$\tilde{H} = \frac{m_1 k_{0,1}}{\mu_{0,1} - m_1} + \frac{m_1(I_{0,1} - \mu_{0,1}) + \mu_{0,1}\alpha_1}{\mu_{0,1}\alpha_1}$$
$$\times \frac{(m_2 + D)k_{1,2}}{\mu_{1,2} - m_2 - D}. \tag{25}$$

Then, the equilibria are

$$\bar{H}^* = x_r, \tag{26}$$

$$\bar{x}_2^* = x_r - \tilde{H}. \tag{27}$$

We conclude that

i)   If $x_r < \hat{H}$ then $(x_1; x_2; p_1; p_2)$ approaches $(0; 0; 0; 0)$,

ii) If $\hat{H} < x_r < \hat{H}$ then $(x_1; x_2; p_1; p_2)$ approaches $(x_1^*; 0; p_1^*; 0)$,

iii) If $\tilde{H} < x_r$ then $(x_1; x_2; p_1; p_2)$ approaches $(x_1^*; x_2^*; p_1^*; 0)$.

Notice that contrary to the batch reactor case, the slow system is now two-dimensional instead of one. In the batch reactor case C serves as a constant while here H is a variable which converges to a constant x_r for time goes to infinity. This mathematical detail has large consequences. The bifurcation diagram Fig. 6 shows that for $D > 0$ the full system becomes unstable when x_r is increased and the Hopf bifurcation curve H_r is passed, while the reduced system where $D = 0$ is assumed in deriving the fast system, has still a stable equilibrium in those situations. Hence the zero-order approximation approach fails when this occurs. Therefore we propose a first-order approximation in the next subsection.

7.2. First-order approximation

The terms proportional to $\varepsilon I_{1,2}$ as well as εD are retained and this yields the first-order approximation. The fast system reduces to the three odes, Eqs. (23b), (23d) and (23e).

The two slow variables $\bar{H}$ and $\bar{x}_2$ are now parameters of the fast system. For small values of x_r there is a stable interior equilibrium. However, when x_r is large the full system has multiple equilibria as a consequence of the predator consumption term proportional to $\varepsilon I_{1,2}$, and this complicates the analysis and therefore we perform a numerical bifurcation analysis where we used locbif. In Kooi et al. (1998) we derived analytic expressions for the chemostat case without recycling and maintenance: $\alpha_i = m_i = 0$, $i = 1, 2$.

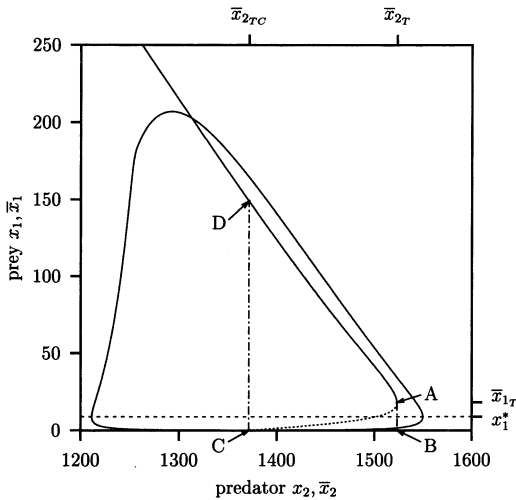The calculated bifurcation one-parameter diagram is shown in Fig. 8 where $x_r = 1600$ and $D =$

Fig. 8. Phase-plane plot for the full system as well as the one-parameter bifurcation diagram of fast system of the model with recycling Eqs. (23a), (23b), (23c), (23d) and (23e) where $x_r = 1600$ mg dm^{-3} and $D = 0.001$ h^{-1}. Values assigned to physiological parameters and reference values for the perturbation parameters are listed in Table 2 for $\varepsilon \ll 1$. The closed solid curve is the limit cycle $(x_1(t), x_2(t))$ for full system. The trajectory ABCD is the quasi-limit cycle for reduced system. Point A indicates a tangent bifurcation point and point C a transcritical bifurcation point, both for the reduced system. Two stable branches of the fast equilibrium manifolds are B → C and D → A. The fast unstable equilibrium manifold curve AC is the separatrix.

0.001. The single bifurcation parameter is the slow variable $\bar{x}_2$. When asymptotic dynamics is concerned, it is sufficient to consider $H(t) = x_r$, (Thieme, 1992; Smith and Waltman, 1994) and since we are mainly interested the long-term dynamics, we took $\bar{H}(t) = x_r$. There are two stable slow manifolds, AD and BC, and one unstable slow manifold, AC. The multiple solutions are the trivial solution $\bar{x}_2 = 0$ and two roots of a quadratic equation obtained by taking the right-hand side of Eq. (23b) equal zero. Observe that the fact that the resulting equation is quadratic in $\bar{x}_1$ results from the predator consumption term proportional to $\varepsilon I_{1,2}$ which was neglected in the zero-order approximation. A transcritical bifurcation, where the graph of the quadratic function crosses the $\bar{x}_1$ axis, is denoted by $\bar{x}_{2_{TC}}$ and a tangent bifurcation, where the discriminant of this quadratic function is zero, is denoted by $\bar{x}_{2_T}$.

Depending on the initial conditions $\bar{x}_1(0)$, $\bar{p}_1(0)$ and $\bar{p}_2(0)$, as well as $\bar{x}_2(0)$, the system converges quickly towards a stable equilibrium of the fast system. When $\bar{x}_2(0) < \bar{x}_{2_{TC}}$ it goes to the positive stable part of the non-trivial branch (left side of D) and when $\bar{x}_2(0) > \bar{x}_{2_T}$ to the stable part of the trivial branch (right side of B).

When $\bar{x}_{2_{TC}} < \bar{x}_2(0) < \bar{x}_{2_T}$ there are two stable equilibria of the fast system. If $\bar{x}_1(0)$ lies below the curve AC in Fig. 8, the system converges quickly to the trivial branch (between B and C). If on the other hand $\bar{x}_1(0)$ lies above the curve AC, the system goes to the non-trivial branch (between A and D). In other words, the unstable fast manifold, curve AC is a separatrix.

When the two parameters x_r and D are so that $\bar{x}_{1_T} < x_1^* = (m_2 + D)k_{1,2}/(\mu_{1,2} - m_2 - D)$ there is a stable equilibrium and both reduced and full system converge when time goes to infinity to this positive equilibrium. If, on the other hand, $\bar{x}_{1_T} > x_1^*$ then the reduced system possesses a quasi-limit cycle, such as the trajectory ABCD in Fig. 8, while the full system shows a limit cycle also shown in Fig. 8. Hence, this figure is also the phase-plane plot for the full system where $x_r = 1600$ and $D = 0.001$.

Observe that generally when $H \neq x_r$ these manifolds move slowly. On the stable trivial fast equilibrium manifold BC the asymptotic dynamics

is described by

$$\frac{\mathrm{d}\bar{H}}{\mathrm{d}t} = -D(\bar{H} - x_r) \tag{28a}$$

$$\frac{\mathrm{d}\bar{x}_2}{\mathrm{d}t} = -D\bar{x}_2, \tag{28b}$$

where $\bar{x}_1 = 0$ and $\bar{p}_1 = 0$ are substituted in Eqs. (23a) and (23c). On the stable non-trivial fast equilibrium manifold DA the dynamics is described by Eqs. (23a) and (23c)

$$\frac{\mathrm{d}\bar{H}}{\mathrm{d}t} = -D(\bar{H} - x_r) \tag{29a}$$

$$\frac{\mathrm{d}\bar{x}_2}{\mathrm{d}t} = \bar{x}_2\left(\mu_{1,2}\frac{\bar{x}_1}{k_{1,2} + \bar{x}_1} - m_2 - D\right), \tag{29b}$$

where $\bar{x}_1$ and $\bar{p}_1$ are the solutions of the equilibrium Eqs. (23b) and (23d).

Subsequently for both the trivial and non-trivial equilibrium manifolds the density of the nutrient, $\bar{x}_0(t)$, may be calculated by the conservation relationship: $\bar{x}_0(t) = x_r - \bar{x}_1(t) - \bar{p}_1(t) - \bar{x}_2(t) - \bar{p}_2(t)$. In Fig. 8 we show these solutions for the reduced system $\bar{x}_1(t)$ and $\bar{x}_2(t)$ as well as the stable limit cycle of the full system $x_1(t)$ and $x_2(t)$.

8. Discussion and conclusions

In this paper we studied the dynamics of a simple food chain where nutrient recycling is taken into account and decomposition is simply modelled as a degradation process. In the literature more realistic models are described and analysed where among others the decomposers are modelled explicitly. We mention two papers where the reader can find these models.

Two types (dissolved and particulate) of nutrients are distinguished in Aota and Nakajima (2000) where they study coexistence of phytoplankton and bacteria with nutrient recycling in a close ecosystem. Phytoplankton can use only dissolved (inorganic) nutrients while the bacteria degrade particulate nutrient (dead bodies of phytoplankton and bacteria) as well. In Kooijman and Nisbet (2000) the complete mass and energy turnover in a daphnids–algae–bacteria (consumers–

producers–decomposers) community in a closed bottle is evaluated. The daphnids consume both algae and bacteria. The algae use solar energy to convert carbon dioxide CO_2 to organic compounds. Different model formulations for the consumers were considered. Bacteria, the decomposers, digest their faeces and those of the algae, and dead *Daphnia*, both instantaneously and completely.

It is expected that the mathematical difficulty in applying aggregation methods for more complex models were decomposers are modelled explicity, are similar to that analysed here. In this paper we refrained from modelling the decomposers since the mathematical difficulty is more transparent, more tractable and similar remedies can be used for the more complex models.

Without maintenance ($m_i = 0$, $i = 1$, 2) and recycling ($\alpha_i = 0$, $i = 1$, 2) Eqs. (10a), (10b), (11a) and (11b) hold and it is easy to derive that all biomass ends finally at the predator level and the other levels are exhausted, see also Kooi et al. (1998). However, in the batch system where maintenance ($m_i > 0$, $i = 1$, 2) and recycling of the nutrient takes place ($\alpha_i > 0$, $i = 1$, 2), evolves to a state where the biomass is distributed over the different trophic levels, see Eqs. (12a), (12b), (12c) and (12d).

In Nisbet et al. (1983b) it is shown that with the Monod model being a special case of the Monod–Herbert model where $m_i = 0$, $i = 1$, 2, the transcritical bifurcation curve TC and the Hopf bifurcation curve H intersect the horizontal axis where $D = 0$. The results for the Monod–Herbert model depicted in Fig. 6, and already given in Nisbet et al. (1983a), show that these bifurcation curves TC and H do not intersect the $D = 0$ axis but approach this axis when x_r goes to infinity. That is a stable equilibrium exists for non-zero, but possibly small, dilution rates. From these results it was concluded in Nisbet et al. (1983a) that maintenance has a stabilising effect. In Fig. 6 the curves TC_r and H_r where maintenance is modelled and also nutrient recycling is taken into account the bifurcation curves intersect the $D = 0$ axis as with the Monod model. Thus, nutrient recycling counteracts the stabilising effect of maintenance.

In Fig. 7 the biomasses are given for the model with and without recycling, that is the Monod–Herbert model. Comparing the results for both models shows that for model Eqs. (23a), (23b), (23c), (23d) and (23e) the oscillations are more severe and at troughs in the cycle the biomasses can become very small. However, when this occurs, the deterministic model formulation fails to hold true and extinction due to demographic stochasticity is likely (Rosenzweig, 1971).

Figs. 3 and 4 illustrate the power of the aggregation technique. After the short transient, the solution of the reduced model is close to that of the full model. The transcritical bifurcations of the reduced model and full model, which terminates invasion of the prey trophic level, occur at exactly the same bifurcation parameter values, $\hat{C}$ and $\tilde{C}$.

For large C-values, however, the time scales have to differ a lot ($\varepsilon \mu_{1,2}/\mu_{0,1} \ll 1$) in order to obtain reasonable approximations. When ε is not small enough, the solution of the full model converges to a stable limit cycle while the solution of the reduced model converges to a stable equilibrium. A first-order approximation approach would give the same qualitative long-term dynamics for both the full and the reduced model.

The zero-order approximation in the chemostat case, indicates a stable equilibrium for the reduced model (where $D = 0$) and a limit cycle for the full model (when $D > 0$ but small). Obviously a hypothesis for applicability of the Fenichel Theorem is not satisfied. This can be explained in biological terms as follows. With $D = 0$ the reservoir, from which the nutrient is supplied into the reactor, is decoupled from the chemostat reactor and the situation resembles the batch reactor case. Hence, the parameter x_r is meaningless when $D = 0$. As a result, as time goes to infinity the total biomass H converges to x_r if $D > 0$, but is time-invariant when $D = 0$. Since in the aggregation approach the dilution rate D is multiplied by the perturbation parameter ε, there is a discontinuity for $\varepsilon = 0$.

The first-order approximation approach gives a better long-term approximation without extra computational efforts for the model studied here. With the first-order approximation reduced model for the chemostat case, the transcritical bifurca-

tions of the reduced model and full model occur at exactly the same bifurcation parameter values. Furthermore, the tangent bifurcation parameter values of the reduced model coincide with those at the Hopf bifurcation of the full system. This implies that the reduced and full model start to oscillate when x_r is increased leaving D unchanged, at exactly the same parameter value.

The differences between the quasi-limit cycle of the reduced system and the limit cycle of the full system shown in Fig. 8 are related to the 'delayed bifurcations' associated with the tangent and transcritical bifurcations of the reduced system, see Diener and Diener (1983), Eckhaus (1983), Schecter (1985), Rinaldi and Muratori (1992b), De Feo and Rinaldi (1998). This phenomenon will be studied in a forthcoming paper.

Observe that we multiplied $I_{1,2}$ with ε in order to get a more biologically realistic model. Hence, there is no complete time-scale separation for the different trophic levels, for the small growth rate of the predator implies a small ingestion rate of the prey. When $I_{1,2}$ is multiplied with ε the dynamics of the fast system is much simpler than without this factor as is assumed in Rinaldi and Muratori (1992a). Unfortunately, the obtained dynamics of the reduced system appears to be too simple under certain circumstances. That is, the reduced system gives not always good approximations for the long-term dynamics, for instance when the initial biomass C is large in the batch reactor case, the reduced system has a stable equilibrium while the full system a stable limit cycle. We showed that also for the chemostat case the asymptotic behaviour of the reduced and full system can differ qualitatively. Hence, as was done by Rinaldi and co-workers, we have take the $\varepsilon I_{1,2}$ term into account with the application of the aggregation technique in order to get good mathematical approximations.

Application of the zero-order approximation perturbation technique does not always yield useful results. We showed that this occurs when the reduced system has a stable equilibrium while the full model possesses a stable limit cycle. In those cases a first-order approximation is needed to get the same qualitative long-term dynamics for both the full and the reduced model. Then, the

reduced system has two slow manifolds and the trajectory follows one slow manifold. When this manifold becomes unstable, the trajectory jumps to the other manifold. The trajectory continues to move along this manifold until it becomes unstable and the trajectory jumps back to the first manifold, and so on and this forms a quasi-limit cycle.

In this article we show how the modelling of food chains and the analysis of the resulting model can be closely related. Bifurcation theory and singular perturbation theory provide tools for the analyse of mathematical models of small-scale ecosystems when different time scales for the trophic levels exist. The reduced model is lower dimensional and is therefore easier to handle analytically and numerically. Numerical simulation of the reduced model requires less computing time important with sensitivity studies and parameter estimation.

References

Aota, Y., Nakajima, H., 2000. Mathematical analysis on coexistence conditions of phytoplankton and bacteria systems with nutrient recycling. Ecological Modelling 135, 17–31.

Auger, P., Poggiale, J.C., 1996. Emergence of population growth models: fast migration and slow growth. Journal of Theoretical Biology 182, 99–108.

Auger, P., Charles, S., Viala, M., Poggiale, J.C., 2000a. Aggregation and emergence of ecological modelling: integration of ecological levels. Ecological Modelling 127, 11–20.

Auger, P., Poggiale, J.C., Charles, S., 2000b. Emergence of individual behaviour at the population level. Effects of density-dependent migration on population dynamics. Comptes rendus de l'Academie des science series III-Sciences de la vie-life 323, 119–127.

Bazykin, A.D., 1998. Nonlinear Dynamics of Interacting Populations. World Scientific, Singapore, p. 216.

Beretta, E., Bischi, G.I., Solimano, F., 1990. Stability in chemostat equations with delayed nutrient recycling. Journal of Mathematical Biology 28, 99–111.

De Feo, O., Rinaldi, S., 1998. Singular homoclinic bifurcations in tri-trophic food chains. Mathematical Biosciences 148, 7–20.

DeAngelis, D.L., 1992. Dynamics of Nutrient Cycling and Food Webs. Number 9 in Population and Community Biology Series. Chapman & Hall, London, p. 270.

Diener, F., Diener, M., 1983. Seven formulas concerning canards. Comptes rendus de l' Academie des science 297, 577–580.

Doedel, E.J., Champneys, A.R., Fairgrieve, T.F., Kuznetsov, Y.A., Sandstede, B., Wang, X., 1997. AUTO 97: Continuation and Bifurcation Software For Ordinary Differential Equations. Technical report. Concordia University, Montreal, Canada.

Dumortier, F., Roussarie, R., 1996. Canard cycles and center manifolds. Memoirs of the American Mathematical Society 577, 1.

Dumortier, F., Roussarie, R., 2000. Geometric singular perturbation theory beyond normal hyperbolicity, In: Jones, C.K.R.T., Khibnik, A.I. (Eds.), Multiple Time Scale Dynamical Systems, vol. 122 of IMA, Springer, Berlin, pp. 29–64.

Eckhaus, W., 1983. Relaxation oscillations including a standard chase on french ducks. In: Asymptotic Analysis II, Lecture Notes in Mathematics, vol. 985. Springer, Berlin.

Fenichel, N., 1971. Persistence and smoothness of invariant manifolds for flows. Indiana University Mathematical Journal 21, 193–226.

Guckenheimer, J., Holmes, P., 1985. Nonlinear Oscillations, Dynamical Systems and Bifurcations of Vector Fields, Applied Mathematical Sciences, vol. 42, second ed.. Springer, New York.

Gurney, W.S.C., Nisbet, R.M., 1998. Ecological Dynamics. Oxford University Press, p. 335.

Hirch, M.W., Pugh, C.C., Shub, M., 1977. Invariant manifolds. Lecture Notes in Biomathematics. Springer, Berlin.

Hoppensteadt, F.C., 1993. Analysis and Simulation of Chaotic Systems. Applied Mathematical Sciences. Springer, Berlin.

Iwasa, Y., Andreasen, V., Levin, S.A., 1987. Aggregation in model ecosystems I. Perfect aggregation. Ecological Modelling 37, 287–302.

Iwasa, Y., Levin, S.A., Andreasen, V., 1989. Aggregation in model ecosystems II. approximate aggregation. IMA Journal of Mathematical Applied Medical Biology 6, 1–23.

Jones, C.K.R.T., 1995. Geometric singular perturbation theory. Dynamical Systems 1609, 44–118.

Kevorkian, J., Cole, J., 1995. Multiple Scale and Singular Perturbation Methods, Applied Mathematical Sciences, vol. 114. Springer, Berlin.

Khibnik, A.I., Kuznetsov, Y.A., Levitin, V.V., Nikolaev, E.V., 1993. Continuation techniques and interactive software for bifurcation analysis of ODEs and iterated maps. Physica D 62, 360–371.

Kooi, B.W., Poggiale, J.C., Auger, P., 1998. Aggregation methods in food chains. Mathematical Computer Modelling 27, 109–120.

Kooijman, S.A.L.M., Nisbet, R.M., 2000. How light and nutrients affect life in a closed bottle. In: Jørgenson, S.E. (Ed.), Thermodynamics and Ecology. CRC Publishers, pp. 19–60.

Kooijman, S.A.L.M., Dijkstra, H.A., Kooi, B.W., 2002. Light-induced mass turnover in a mono-species community of mixotrophs. Journal of Theoretical Biology 214, 233–254.

Kooijman, S.A.L.M., 2000. Dynamic Energy and Mass Budgets in Biological Systems. Cambridge University Press, Cambridge.

Kuznetsov, Y.A., 1998. Elements of Applied Bifurcation Theory, Applied Mathematical Sciences, vol. 112, second ed.. Springer, New York.

Kuznetsov, Y.A., Levitin, V.V., 1997. CONTENT: Integrated environment for the analysis of dynamical systems. Centrum voor Wiskunde en Informatica (CWI), Kruislaan 413, 1098 SJ Amsterdam, The Netherlands, 1.5 ed.

Muratori, S., Rinaldi, S., 1989. A dynamical system with hopf bifurcations and catastrophes. Applied Mathematics Computation 29, 1–15.

Muratori, S., Rinaldi, S., 1992. Low- and high-frequency oscillations in three-dimensional food chain systems. SIAM Journal of Applied Mathematics 52, 1688–1706.

Nisbet, R.M., Gurney, W.S.C., 1976. Model of material cycling in a closed ecosystem. Nature 264, 633–634.

Nisbet, R.M., Cunningham, A., Gurney, W.S.C., 1983a. Endogenous metabolism and the stability of microbial prey–predator systems. Biotechnology and Bioengineering 25, 301–306.

Nisbet, R.M., McKinstry, J., Gurney, W.S.C., 1983b. A strategic model of material cycling in a closed ecosystem. Mathematical Biosciences 64, 99–113.

Poggiale, J.C., Auger, P., 1996. Fast oscillating migrations in a predator–prey model. Mathematical Models and Methods in Applied Sciences (M3AS) 6, 217–226.

Ratsak, C.H., Kooijman, S.A.L.M., Kooi, B.W., 1993. Modelling the growth of an oligocheate on activated sludge. Water Research 27, 739–747.

Rinaldi, S., Muratori, S., 1992a. Limit-cycles in slow fast forest pest models. Theoretical Population Biology 41, 26–43.

Rinaldi, S., Muratori, S., 1992b. Slow fast limit-cycles in predator prey models. Ecological Modelling 61, 287–308.

Rosenzweig, M.L., 1971. Paradox of enrichment: destabilization of exploitation ecosystems in ecological time. Science 171, 385–387.

Ruan, S., 1993. Persistence and coexistence in zooplankton–phytoplankton–nutrient models with instantaneous nutrient recycling. Journal of Mathematical Biology 31, 633–654.

Ruan, S., 2001. Oscillations in plankton models nutrient recycling. Journal of Theoretical Biology 208, 15–26.

Schecter, S., 1985. Persistent unstable equilibria and closed orbits of a singularly perturbed equation. Journal of Diffusional Equation 60, 131–141.

Smith, H.L., Waltman, P., 1994. The Theory of the Chemostat. Cambridge University Press, Cambridge, p. 313.

Thieme, H.R., 1992. Convergence results and a Poincaré-Bendixon trichotomy for asymptotically autonomous differential equations. Journal of Mathematical Biology 30, 755–763.

Tikhonov, A.N., Vasil'eva, A.B., Sveshnikov, A.G., 1985. Differential Equations. Lecture Notes in Biomathematics. Springer, Berlin.

Wiggins, S., 1994. Normally Hyperbolic Invariant Manifolds in Dynamical Systems. Applied Mathematical Sciences. Springer, New York, p. 105.